第 35 卷第 6 期
2019 年 6 月

无 机 化 学 学 报
CHINESE JOURNAL OF INORGANIC CHEMISTRY

Vol.35 No.6
1065-1075

基于 *D*(−)/*L*(+)-对羟基苯甘氨酸配体的两个铜配合物的合成、结构和电化学性质

刘曼玉　史亚静　王兰芝　宋会花*

(河北师范大学化学与材料科学学院,石家庄　050024)

摘要：利用手性配体 *D*(−)/*L*(+)-对羟基苯甘氨酸(*D*/*L*-Hhpg)与铜盐在溶液法条件下合成 2 个手性配合物{[Cu(*D*-hpg)(phen)(NO_3)]·1.5H_2O}$_n$ (**1**)和{[Cu(*L*-hpg)(phen)(NO_3)]·2H_2O}$_n$(**2**),(phen=1,10-菲咯啉)。对 2 个配合物进行了元素分析、红外光谱、粉末 X 射线衍射、单晶 X 射线衍射、固态圆二色谱表征及热重−差热分析。配合物 **1** 和 **2** 是正交晶系,$P2_12_12_1$ 手性空间群,二者均为 1D 链状结构并通过氢键作用形成 3D 超分子结构。有趣的是,配合物 **1** 和 **2** 中的配位硝酸根与晶格水分子之间的氢键作用使它们分别生成了沿 *b* 轴方向的左手和右手超分子螺旋链。此外,基于配合物 **1** 和 **2** 的中心金属离子为 Cu(Ⅱ),进一步探究了电化学性能。循环伏安结果表明生成的配合物具有电化学活性,在扫描速率为 0.025~1.0 V·s^{-1} 范围内,配合物制备的碳糊电极上的电化学过程是由表面控制的。

关键词：*D*(−)/*L*(+)-对羟基苯甘氨酸；晶体结构；手性配合物；电化学

中图分类号：O614.121　　**文献标识码**：A　　**文章编号**：1001-4861(2019)06-1065-11

DOI:10.11862/CJIC.2019.130

Syntheses, Crystal Structures and Electrochemical Properties of Two Chiral Cu Complexes Based on *D*(−)/*L*(+)-4-Hydroxyphenylglycine

LIU Man-Yu　SHI Ya-Jing　WANG Lan-Zhi　SONG Hui-Hua*

(*College of Chemistry and Material Sciences, Hebei Normal University, Shijiazhuang* 050024, *China*)

Abstract: Two chiral coordination compounds based on *D*(−)/*L*(+)-4-hydroxyphenylglycine (*D*/*L*-Hhpg), {[Cu(*D*-hpg)(phen)(NO_3)]·1.5H_2O}$_n$ (**1**) and {[Cu(*L*-hpg)(phen)(NO_3)]·2H_2O}$_n$ (**2**) (phen=1,10-phenanthroline) have been synthesized and characterized by elemental analysis, infrared spectroscopy, powder X-ray diffraction, single-crystal X-ray diffraction, solid-state CD spectra and TG-DSC analysis. Compounds **1** and **2** are orthorhombic, $P2_12_12_1$ chiral space groups. They are 1D chain structure, which is extended into a 3D supramolecular structure by the hydrogen bond. Interestingly, the compounds **1** and **2** exist left-handed or right-handed supramolecular helix chains along the *b* axis direction by the hydrogen bond respectively, which is extended by the hydrogen bond between coordinated nitrate anion and lattice water. Furthermore, based on the central metal ions of Cu(Ⅱ), further explored the compounds **1** and **2** of electrochemical properties, Analysis of cyclic voltammetry at varying scan rates (0.03 to 0.13 V·s^{-1}) demonstrates a linear relationship between the anode peak current and the scan rate, indicating a surface-controlled electrochemical process. CCDC: 1440300, **1**; 1505353, **2**.

Keywords: *D*(−)/*L*(+)-4-hydroxyphenylglycine; crystal structure; homochiral coordination compounds; electrochemistry

收稿日期:2018-08-09。收修改稿日期:2019-04-13。

国家自然科学基金(No.21776060)、河北省自然科学基金(No.B2018205152)、河北师范大学应用开发基金(No.L2016K03)和河北省引进留学人员资助项目(No.CL201715)资助。

*通信联系人。E-mail:songhuihua@mail.hebtu.edu.cn

0 Introduction

Currently, there has been increasing interest in creating of chiral compounds due to their potential applications, such as gas adsorption, catalysis, drug delivery, separation, fluorescence, non-linear optics[1-10]. Chiral coordination polymers endued with plentiful structure, ultrahigh surface area and tunable ability should be regarded as promising potential chiral sensors[11-15]. Cyclic voltammogram (CV) technique provides highly selective, and fast speed operation, which be regarded as promising tool for exploring redox properties and chiral recognition[16-18]. Generally, the predictable syntheses of chiral coordination frameworks have been accomplished in the following three ways: (i) using the chiral ligands as a linker to connect metal ions [19]; (ii) using achiral ligands under spontaneous resolution induced by chiral auxiliary[20]; (iii) using the racemic organic ligands to self-assemble with metal ions in spontaneous resolution[21]. However, the relative ease of formation by self-assembly usually be effected by many factors such as solvent system, ligand-to-metal ratios, temperature, metal ions, pH value of solution[22-27]. Hence, the controllable synthesis of stable chiral coordination compounds becomes one of the most burdensome challenges to chemists.

In the above methods, using the chiral ligands as a linker to construct chiral coordination compounds is the most effective method. Some optically active amino acid molecules with chiral centers such as *L*-glutamic acid, *L*-tartric acid, *L*-lactic acid, and organic ligands containing chiral polypyridyl or polycarboxylate groups, have already been widely used to obtain artificial chiral compounds[28-34]. *D*(−)/*L*(+)-4-Hydroxyphenylglycine (*D*/*L*-Hhpg) have both amino and carboxyl functional groups, and as ligands they can coordinate metal ions by monodentate, bidentate, chelating and bridging mode. A literature survey revealed that examples of complexes based on *D*/*L*-Hhgp are sparse. Only a few examples of chiral cyclic assemblies have been reported to date. Ivan Bernal et al.[35] have reported [Cu(4HPG)(bpy)]·$2H_2O$ compounds (4HPG= *D*-4-hydroxyphenylglycinato, bpy=2,2′-bipyridine), and in 2015 the related compound $[Cu(hpg)_2(H_2O)]_n$ was synthesized by the group of Yao[36]. Our laboratory have reported three enantiomeric pairs of chiral coordination compounds, namely $\{[Zn(D\text{-hpg})(4,4'\text{-bipy})(H_2O)]NO_3\}_n$, $\{[Zn(L\text{-hpg})(4,4'\text{-bipy})(H_2O)]NO_3\}_n$, $\{[Zn(D\text{-hpg})(4,4'\text{-bipy})(H_2O)]ClO_4\}_n$, $\{[Zn(L\text{-hpg})(4,4'\text{-bipy})(H_2O)]ClO_4\}_n$, $[Zn(D\text{-hpg})_2(4,4'\text{-bipy})]\cdot 2(4,4'\text{-bipy})\cdot H_2O$, $[Zn(L\text{-hpg})_2(4,4'\text{-bipy})]\cdot 2(4,4'\text{-bipy})\cdot H_2O$ (4,4′-bipy=4,4′-bipyridine), and discussed how the metal salts and pH value affect the structures and properties of the compounds[37].

In this work two chiral coordination compounds assembled from copper salts and *D*/*L*-Hhpg, $\{[Cu(D\text{-hpg})(phen)(NO_3)]\cdot 1.5H_2O\}_n$ (**1**) and $\{[Cu(L\text{-hpg})(phen)(NO_3)]\cdot 2H_2O\}_n$ (**2**) (phen=1,10-phen-anthroline), were successfully synthesized and struc-turally characterized. Their crystal structures, TG-DTA analysis and cyclic voltammetry are discussed in detail.

1 Experimental

1.1 Materials and methods

All reagents and solvents for syntheses were purchased from commercial sources and were used as received without further purification. Element analyses (C, H and N) were performed on an Elemental Vario EL elemental analyzer. Infrared (IR) spectra were measured on a FTIR-8900 spectrometer from 4 000 to 400 cm^{-1} (KBr pellets). Thermogravimetry-differential scanning calorimetry (TG-DSC) experiments were carried out on a simultaneous STA 449F3/TENSOR 27 thermal analyzer under a static N_2 atmosphere with a heating rate 10 ℃·min^{-1} from room temperature to 850 ℃. Powder X-ray diffraction (PXRD) patterns were collected on a Bruker D8-Advance X-ray diffractometer using Cu $K\alpha$ radiation (λ=0.154 2 nm, U=40 kV, I=40 mA) in 2θ range of 5°~50° at room temperature. The solid state circular dichroism (CD) spectra were recorded on a JASCOJ-810 spectropolari-meter with KCl pellets. Cyclic voltammetry measurements were carried out on a CHI 660 electrochemical workstation at room temperature. Platinum gauze was used as a counter electrode, and a saturated calomel electrode (SCE) was used as reference electrode. Chemically

bulk-modified carbon paste electrodes (CPEs) were used as the working electrodes. The compound (**1** and **2**) modified CPEs (**1**/**2**-CPE) was fabricated as follows: 0.1 g of graphite powder and 0.01 g of (**1** and **2**) were mixed and ground together by an agate mortar and pestle to achieve a uniform mixture and then 0.1 mL paraffin oil was added with stirring. The homogenized mixture was packed into a plastic tube with a 2 mm inner diameter. Electrical contact was established with a copper rod through the back of electrode.

1.2 Synthesis

1.2.1 $\{[Cu(D\text{-hpg})(phen)(NO_3)]\cdot 1.5H_2O\}_n$ (**1**)

$Cu(NO_3)_2\cdot 3H_2O$ (0.024 1 g, 0.1 mmol), *D*-Hhpg (0.016 7 g, 0.1 mmol) was stirred into a 10 mL aqueous solution. A solution of phen (0.019 8 g, 0.1 mmol) in EtOH (6 mL) was slowly added. The resulting solution was stirred for 20 minutes, The pH value of solution was adjusted to 4.8 with 1 mol·L^{-1} NaOH solution, and the blue block-shaped transparent crystals **1** suitable for X-ray analysis were obtained with 66% yield based on Cu. Anal. Calcd. For $C_{20}H_{19}N_4O_{7.5}Cu$ (%): C, 48.14; H, 3.83; N, 11.22. Found(%): C, 48.03; H, 3.91; N, 11.00. IR (KBr, cm^{-1}): 3 417 (w), 3 286 (s), 3 232 (m), 1 635 (s), 1 519 (m), 1 465 (w), 1 427 (m), 1 388 (s), 1 327 (s), 1 249 (m), 1 141 (m), 1 103 (w), 1 018 (m), 848 (m), 833 (m), 794 (w), 725 (m), 609 (w), 570 (w)。

1.2.2 $\{[Cu(L\text{-hpg})(phen)(NO_3)]\cdot 2H_2O\}_n$ (**2**)

Compound **2** was synthesized in a procedure similar to that for **1** except that *L*-Hhpg (0.016 7 g, 0.1 mmol) was used instead of *D*-Hhpg (0.016 7 g, 0.1 mmol). The blue block-shaped transparent crystals of **2** were obtained with 62% yield based on Cu. Anal. Calcd. for $C_{20}H_{20}N_4O_8Cu$(%): C, 47.29; H, 3.96; N, 11.03. Found(%): C, 47.73; H, 3.91; N, 11.29. IR (KBr, cm^{-1}): 3 417 (w), 3 286 (s), 3 232 (m), 1 635 (s), 1 519 (m), 1 465 (w), 1 427 (m), 1 388 (s), 1 327 (s), 1 249 (m), 1 141 (m), 1 103 (w), 1 018 (m), 848 (m), 833 (m), 794 (w), 725 (m), 609 (w), 570 (w).

1.3 X-ray crystallography

Single-crystal X-ray crystals for title compounds were selected for single-crystal diffraction analyses (Crystal size: 0.31 mm×0.20 mm×0.15 mm for **1**; 0.29 mm×0.18 mm×0.12 mm for **2**). The data for **1** and **2** were collected on a Bruker SMART-CCD diffractometer by φ-ω scan mode. The structure was solved through direct methods using SHELXS-97 and all non-hydrogen atoms were refined anisotropically by full-matrix least-squares on F^2 using SHELXL-97[38]. Further crystallographic data and experimental details for structural analyses of compounds **1** and **2** are summarized in Table 1.

CCDC: 1440300, **1**; 1505353, **2**.

Table 1　Crystal data and structure refinements for 1 and 2

Compound	1	2
Empirical formula	$C_{40}H_{38}N_8O_{15}Cu_2$	$C_{20}H_{20}CuN_4O_8$
Temperature / K	136.38(10)	100.00(10)
Formula weight	997.86	507.94
Wavelength / nm	0.154 184	0.071 073
Space group	$P2_12_12_1$	$P2_12_12_1$
Crystal system	Orthorhombic	Orthorhombic
a / nm	0.670 680(11)	0.660 805(13)
b / nm	1.602 33(3)	1.584 88(4)
c / nm	1.901 50(3)	1.898 20(4)
V / nm^3	2.043 45(6)	1.987 98(7)
Z	2	4
D_c / (g·cm^{-3})	1.622	1.697
F(000)	1024	1044
Limiting indices	$-4 \leqslant h \leqslant 8, -17 \leqslant k \leqslant 19, -11 \leqslant l \leqslant 22$	$-8 \leqslant h \leqslant 5, -19 \leqslant k \leqslant 17, -16 \leqslant l \leqslant 23$

Continued Table 1

Reflection collected, unique	4 754, 3 186 (R_{int}=0.013 3)	5 248, 3 294 (R_{int}=0.022 4)
Completeness to θ / %	99.7	99.7
Max. and min. transmission	1.000 00 and 0.824 28	1.000 00 and 0.995 98
Data, restraint, parameter	3 186, 0, 299	3 294, 0, 305
GOF	1.058	1.063
R_1, wR_2 [$I>2\sigma(I)$]	0.029 7, 0.099 2	0.033 2, 0.083 5
R_1, wR_2 (all data)	0.031 9, 0.100 6	0.036 1, 0.085 2
Absolute structure parameter	–0.01(3)	0.000(14)
Largest diff. peak and hole / (e·nm^{-3})	–290 and –410	317 and –492
Flack parameter	–0.01(3)	0.000(14)

2 Results and discussion

2.1 Crystal structure

Single crystal X-ray diffraction analysis revealed that compound **1** crystallizes in the Orthorhombic space group of $P2_12_12_1$ and possesses a 1D chain structure. As shown in Fig.1, the asymmetric unit is composed of one Cu(Ⅱ) cation, one *D*-hpg$^-$ anion, one phen ligand, one and a half coordinated water molecule and one nitrate counter anion. Each Cu(Ⅱ) exhibits a distorted octahedral geometry, which is six-coordinated by three oxygen atoms (O1, O6, O7) from one *D*-hpg$^-$ anion and two nitrate counter anions, and nitrogen atoms (N3, N1, N2) from one *D*-hpg$^-$ anion and one phen ligand. The O1, N1, N2 and N3 atoms form the equatorial plane, O6 and O7 atoms occupy the apical positions. The Cu-O bond lengths are 0.192 3(2) and 0.262 0(3) nm, and the Cu-N bond lengths range are between 0.199 9(2) and 0.201 3(3) nm, which are in accordance with the previously reported complexes[39]. Selected bond lengths and angles are given in Table 2.

For compound **1**, nitrate counter anion bridges two Cu(Ⅱ) ions through two different oxygen atoms (O6, O7) to form a 1D infinite linear structure along the *a*-axis direction. As shown in Fig.2, the 1D chains are stacked in an ABAB fashion along the *b*-axis direction with the shortest Cu-Cu distance between adjacent chains being 0.867 54(7) nm. *D*-hpg$^-$ and phen coordinate with Cu^{2+} in bidentate chelate coordination mode as modifying ligands, and arrange on both sides of the chain. It is worth noting that these chains are further extended through extensive

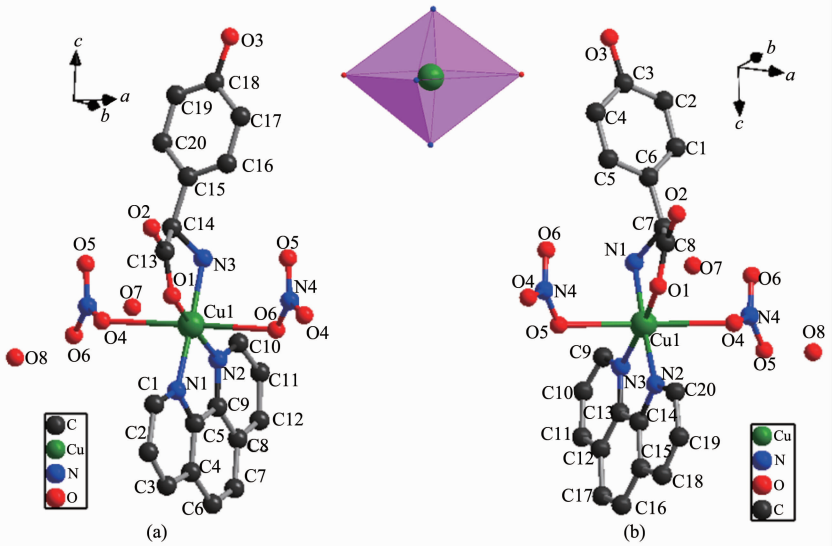

H atoms have been omitted for clarity

Fig.1 Coordination environment of Cu(Ⅱ) for **1** (a) and **2** (b)

hydrogen bonding interactions (Table 3): (1) hydrogen bonding between lattice water and lattice water (O(8)⋯O(7)#5 0.308 3(7) nm); (2) hydrogen bonding between lattice water and coordinated carboxyl oxygen atom (O(7)⋯O(1)#4 0.314 9(4) nm); (3) hydrogen bonding between lattice water and uncoordinated carboxyl oxygen atom (O(7)⋯O(2)#4 0.276 2(4) nm); (4) hydrogen bonding between lattice water and phenol hydroxyl oxygen atom (O(3)⋯O(7)#3 0.263 7(4) nm); (5) hydrogen bonding between the amino nitrogen atom of the coordination and the phenolic hydroxyl oxygen atom of another molecule (N(3)⋯O(3)#2 0.309 2(4) nm); (6) hydrogen bonding between the coordinated amino nitrogen atom and the coordinated nitrate anion

Table 2　Selected bond distances (nm) and angles (°) for compound 1

Cu(1)-O(1)	0.192 3(2)	Cu(1)-N(1)	0.200 5(2)	Cu(1)-O(4)	0.262 0(3)
Cu(1)-N(3)	0.199 9(2)	Cu(1)-N(2)	0.201 3(3)		
O(1)-Cu(1)-N(3)	83.74(9)	N(3)-Cu(1)-O(4)	92.52(12)	C(14)-N(3)-Cu(1)	107.17(17)
O(1)-Cu(1)-N(1)	94.13(9)	N(1)-Cu(1)-O(4)	85.88(10)	Cu(1)-N(3)-H(3A)	110.3
N(3)-Cu(1)-N(1)	177.42(11)	N(2)-Cu(1)-O(4)	100.13(11)	Cu(1)-N(3)-H(3B)	110.3
O(1)-Cu(1)-N(2)	172.61(11)	C(1)-N(1)-Cu(1)	129.5(2)	C(13)-O(1)-Cu(1)	116.1(2)
N(3)-Cu(1)-N(2)	99.58(10)	C(5)-N(1)-Cu(1)	111.74(19)	N(4)-O(4)-Cu(1)	124.7(2)
N(1)-Cu(1)-N(2)	82.71(10)	C(10)-N(2)-Cu(1)	130.3(2)		
O(1)-Cu(1)-O(4)	86.26(11)	C(9)-N(2)-Cu(1)	111.2(2)		

Table 3　Hydrogen bond parameters for compound 1

D–H⋯A	*d*(D-H) / nm	*d*(H⋯A) / nm	*d*(D⋯A) / nm	∠DHA / (°)
O(7)–H(7A)⋯O(6)	0.085	0.197	0.281 7(4)	172.9
O(8)–H(8A)⋯O(4)	0.085	0.226	0.308 4(7)	162.6
N(3)–H(3A)⋯O(5)#1	0.090	0.247	0.316 3(4)	133.7
N(3)–H(3B)⋯O(3)#2	0.090	0.219	0.309 2(4)	174.9
O(3)–H(3C)⋯O(7)#3	0.082	0.182	0.263 7(4)	176.1
O(7)–H(7B)⋯O(2)#4	0.085	0.192	0.276 2(4)	170.8
O(7)–H(7B)⋯O(1)#4	0.085	0.253	0.314 9(4)	130.7
O(8)–H(8B)⋯O(7)#5	0.085	0.226	0.308 3(7)	160.4

Symmetry codes: #1: *x*+1, *y*, *z*; #2: *x*−1/2, −*y*+3/2, −*z*+1; #3: *x*+1/2, −*y*+3/2, −*z*+1; #4: −*x*+1, *y*+1/2, −*z*+1/2; #5: −*x*, *y*−1/2, −*z*+1/2.

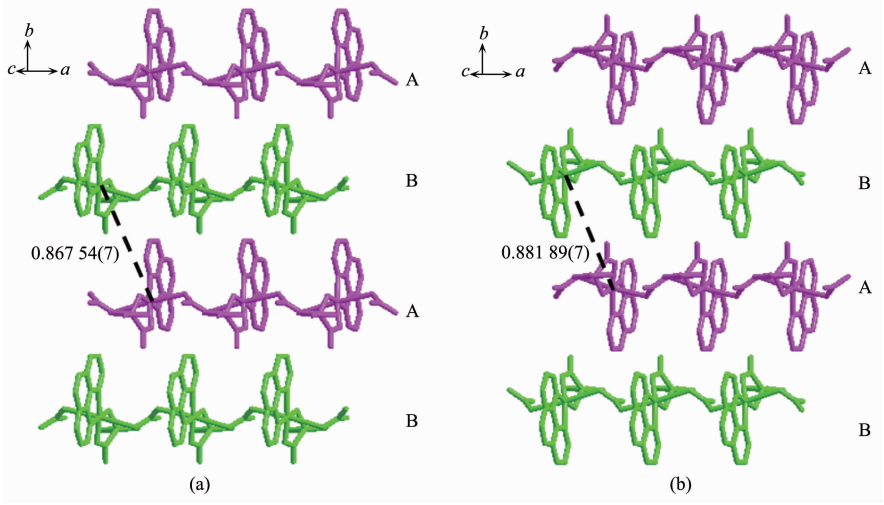

Fig.2　ABAB stacking along *b* axis for **1** (a) and **2** (b)

oxygen atom (N(3)···O(5)#1 0.316 3(4) nm); (7) hydrogen bonding between lattice water and coordinated nitrate anion oxygen atom (O(7)···O(6) 0.281 7(4) nm, O(8)···O(4) 0.308 4(4) nm). Interestingly, between lattice water molecules and coordination nitrate anions there exist extensive hydrogen bonds(O(7)···O(6) 0.281 7(4) nm, O(8)···O(4) 0.308 4(4) nm, O(8)···O(7)#5 0.308 3(7) nm)resulting in a 1D left-handed helical chain along the *b*-axis direction (Fig.3). The adjacent chain form weak π-π stacking interaction through the phen ligand (Fig.4). The combination of hydrogen bonding and π-π stacking makes the 3D supramolecular structure of the compounds more stable.

By comparing the crystallography data of **1** and **2** showed in Table 1 as well as Fig.1a and Fig.1b, their different chirality is caused by the different chirality of main ligands, namely *D*-Hhpg and **L**-Hhpg. As shown in Fig.3b, the difference of their crystal structures is that *L*-hpg$^-$ ligands form right-handed supramolecular helices along the *b*-axis for **2** by the extensive hydrogen bond between lattice water molecules and coordination nitrate anion (O(7)···O(5)#2

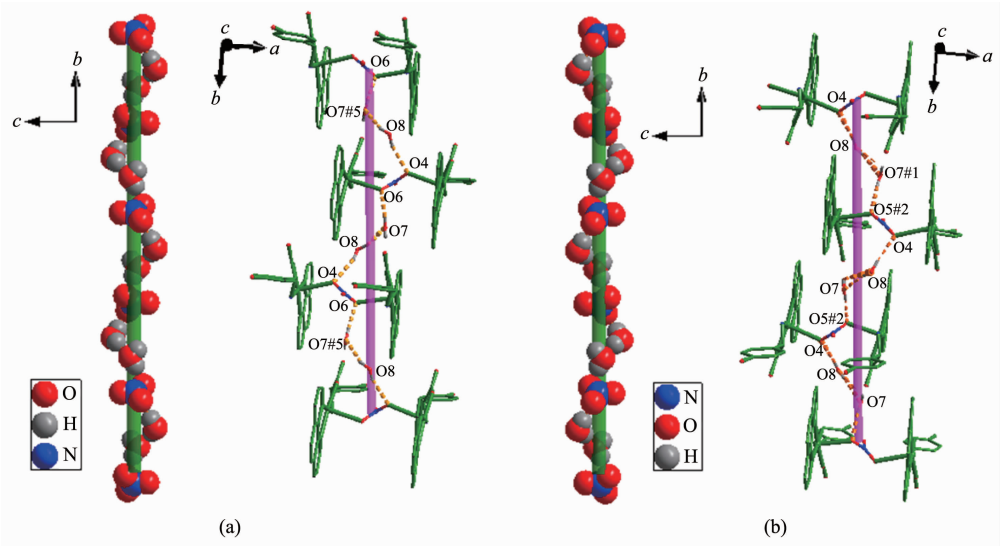

Symmetry codes: #5: $-x$, $y-1/2$, $-z+1/2$ for **1**; #1: $x+1$, y, z; #2: $-x+1$, $y+1/2$, $-z+1/2$ for **2**

Fig.3 (a) One dimensional left-handed double stranded helices of compound **1**; (b) One dimensional right-handed double stranded helices of compound **2**

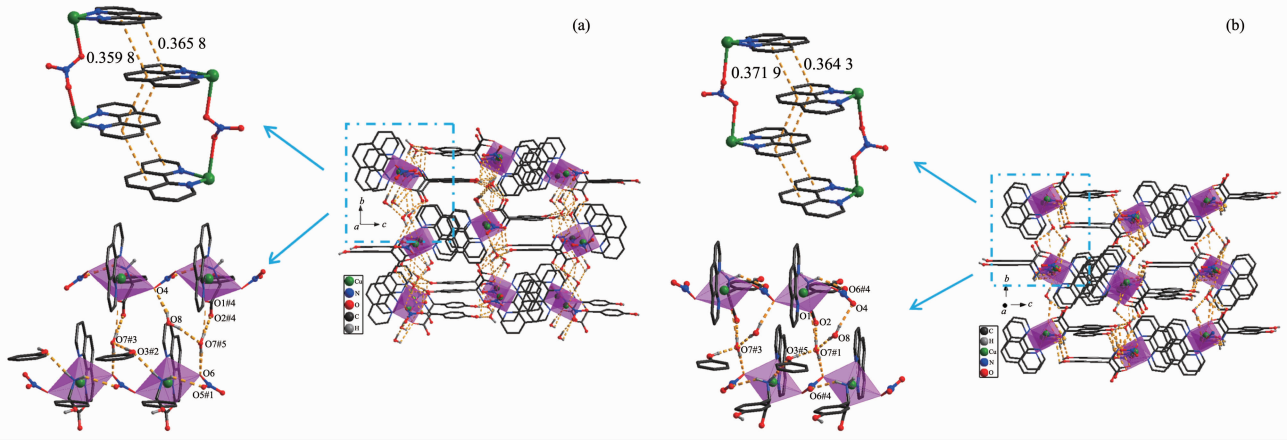

Symmetry codes: #1: $x+1$, y, z; #2: $x-1/2$, $-y+3/2$, $-z+1$; #3: $x+1/2$, $-y+3/2$, $-z+1$; #4: $-x+1$, $y+1/2$, $-z+1/2$; #5: $-x$, $y-1/2$, $-z+1/2$ for **1**; #1: $x+1$, y, z; #2: $-x+1$, $y+1/2$, $-z+1/2$; #3: $-x+1/2$, $-y+1$, $z-1/2$; #4: $x-1$, y, z; #5: $x+1/2$, $-y+1/2$, $-z$ for **2**

Fig.4 Three dimensional supramolecular layers formed by hydrogen bonding and π-π stacking for **1** (a) and **2** (b)

0.278 1(4) nm, O(8)⋯O(7)#1 0.299 1(5) nm, O(8)⋯O(4) 0.303 9(5) nm; Table 4). In addition, the Cu-O bond lengths are 0.192 5(2) and 0.261 3(2) nm, and the Cu-N bond lengths are 0.199 6(3) and 0.200 7(3) nm for **2**. Selected bond lengths and angles are given in Table 5.

Table 4　Hydrogen bond parameters for compound 2

D–H⋯A	*d*(D-H) / nm	*d*(H⋯A) / nm	*d*(D⋯A) / nm	∠DHA / (°)
O(8)–H(8A)⋯O(7)#1	0.085	0.215	0.299 1(5)	169.7
O(8)–H(8B)⋯O(4)	0.085	0.219	0.303 9(5)	173.8
O(7)–H(7B)⋯O(5)#2	0.085	0.194	0.278 1(4)	172.6
O(7)–H(7A)⋯O(1)	0.085	0.250	0.311 5(4)	129.8
O(7)–H(7A)⋯O(2)	0.085	0.190	0.274 1(3)	171.3
O(3)–H(3)⋯O(7)#3	0.082	0.181	0.263 1(4)	174.9
N(1)–H(1B)⋯O(6)#4	0.090	0.241	0.310 4(4)	133.6
N(1)–H(1A)⋯O(3)#5	0.090	0.215	0.304 6(4)	174.3

Symmetry codes: #1: *x*+1, *y*, *z*; #2: −*x*+1, *y*+1/2, −*z*+1/2; #3: −*x*+1/2, −*y*+1, *z*−1/2; #4: *x*−1, *y*, *z*; #5: *x*+1/2, −*y*+1/2, −*z*.

Table 5　Selected bond distances (nm) and angles (°) for compound 2

Cu(1)-O(1)	0.192 5(2)	Cu(1)-N(1)	0.199 6(3)	Cu(1)-O(4)	0.261 3(2)
Cu(1)-N(2)	0.199 6(3)	Cu(1)-N(3)	0.200 7(3)		
O(1)-Cu(1)-N(2)	93.92(10)	N(2)-Cu(1)-O(4)	86.14(10)	Cu(1)-N(1)-H(1A)	110.3
O(1)-Cu(1)-N(1)	83.77(10)	N(1)-Cu(1)-O(4)	92.02(11)	Cu(1)-N(1)-H(1B)	110.3
N(2)-Cu(1)-N(1)	177.15(12)	N(3)-Cu(1)-O(4)	101.26(10)	C(9)-N(3)-Cu(1)	130.2(2)
O(1)-Cu(1)-N(3)	172.17(12)	C(8)-O(1)-Cu(1)	116.0(2)	C(13)-N(3)-Cu(1)	111.4(2)
N(2)-Cu(1)-N(3)	82.89(11)	C(20)-N(2)-Cu(1)	129.5(2)	C(9)-N(3)-Cu(1)	130.2(2)
N(1)-Cu(1)-N(3)	99.61(11)	C(14)-N(2)-Cu(1)	112.0(2)	N(4)-O(4)-Cu(1)	121.75(19)
O(1)-Cu(1)-O(4)	85.61(10)	C(7)-N(1)-Cu(1)	107.21(19)		

2.2　Powder X-ray diffraction analyses and IR spectra

The PXRD patterns for **1** and **2** are presented in Fig.5. The main peaks of simulated spectra of **1** and **2** matched well with their experimental spectra, demonstrating the crystallization degree and the purity of crystalline phase are both good. The ν_{as}(COO−) and ν_s(COO−) vibrations of *D*-hpg$^-$/*L*-hpg$^-$ can be observed

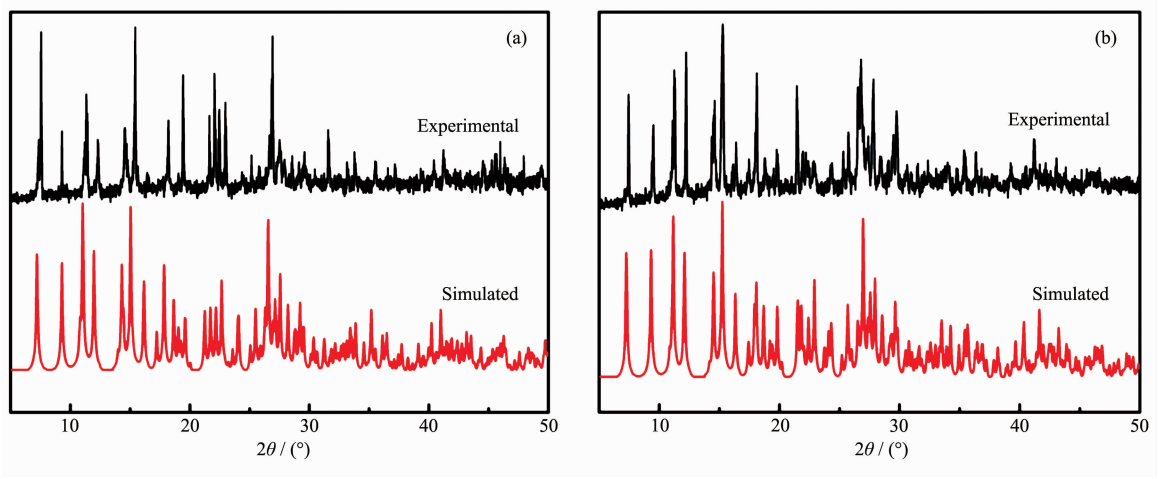

Fig.5　PXRD patterns for **1** (a) and **2** (b)

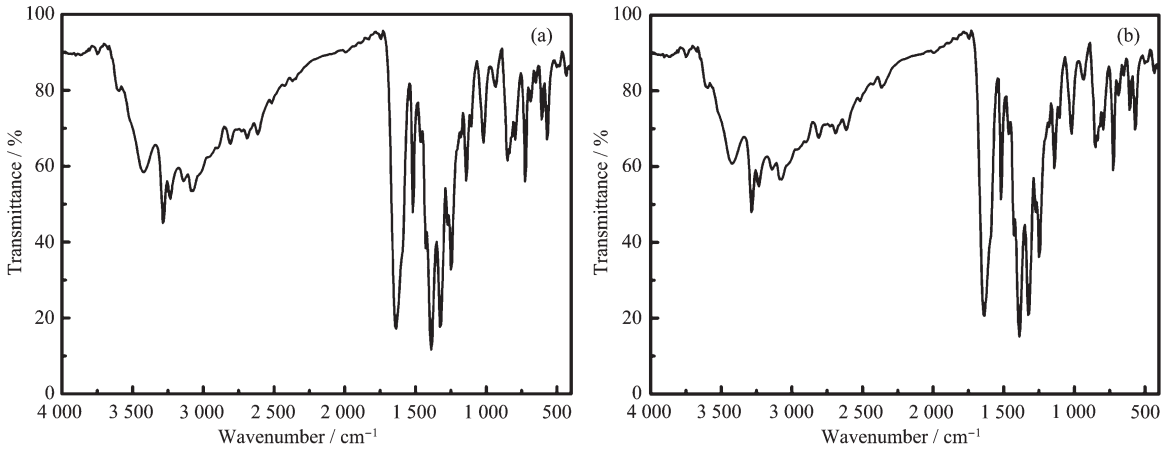

Fig.6 IR spectra of **1** (a) and **2** (b)

at 1 635 and 1 427 cm^{-1}. The peak at 1 249 cm^{-1} is due to ν(C-O) vibrations of phenolic hydroxyl group, and the peaks at 1 327 cm^{-1} are due to ν_{as}(C-N) vibrations of amino-groups which connect to the carbon atoms in amino-acids. The (C-C) and (C=N) vibrations of phen can be observed at 1 519 and 1 388 cm^{-1}, which had a certain degree of red-or blue-shift compared to the related absorption peak of phen at 1 504 and 1 419 cm^{-1}, respectively. Meanwhile, the (C-H) bending vibration of phen at 840 and 732 cm^{-1} have moved to 848 and 725 cm^{-1}, respectively. This result indicates that the phen molecules have coordinated with metal. In addition, the strong peaks at 3 244~3 348 cm^{-1} are due to ν(N-H) vibrations of *D*-hpg$^-$/*L*-hpg$^-$ ligands (Fig.6).

2.3 Circular dichroism spectra properties

The solid-state circular dichroism (CD) spectra of compounds **1** and **2** were investigated at room temperature, as shown in Fig.7. Chiral ligand *D*-Hhpg displayed positive peak value at 245, 261 and 283 nm, while *L*-Hhpg displayed negative peak value at 240, 268 and 284 nm. Compound **1** displayed negative peak value at 237, 275 and 305 nm, and compound **2** displays positive peak value at 254, 282 and 306 nm. From the CD spectra, we can clearly see that **1** and **2** both show obvious Cotton effect, which confirms the two compounds are chiral compounds. Besides the opposite CD signal in the same peak position from compounds **1** and **2**, we can come up with a conclusion is that their CD spectra are image symmetrical, while the CD signal direction of the compound is affected by chiral ligands (Fig.7).

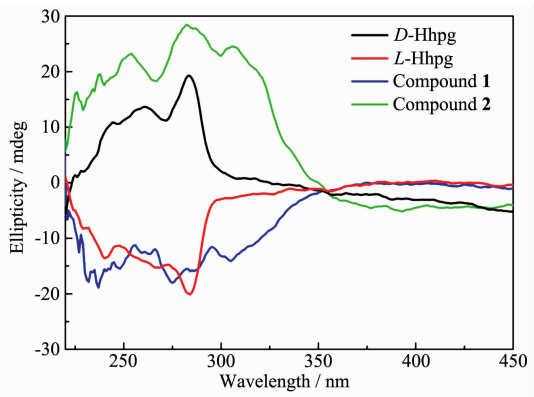

Fig.7 Solid-state CD spectra of *D*-Hhpg/*L*-Hhpg and compounds **1** and **2**

2.4 Thermal analyses

The TG/DTG-DSC methods were used to describe thermal decomposition of synthesized compounds in air as shown in the Fig.8. The thermal decomposition results are presented in Table 6. Compound **1** is fairly stable before 121.37 ℃. The first weight loss in a temperature range of 121.37~181.37 ℃ is consistent with the removal of one and a half lattice water molecules (Obsd. 4.55%, Calcd. 5.41%). On the DSC curve, endothermic peak was observed at about 173.37 ℃, which can prove the loss of one and a half lattice water molecules. The second and third decomposition steps occurred in a temperature range of 181.37~251.37 ℃ and 251.37~481.15 ℃ with a weight loss of 21.49% and 24.51%, respectively, against calculated weight loss of 45.32%, corresponding to the loss of *D*-Hhpg and part of nitrate anion. There

Table 6　Thermal decomposition data for compounds 1 and 2

Compound	Step	Temperature range / ℃	$T_{p,DTG}$ / ℃	Weight loss / %		$T_{p,DSC}$ / ℃	Probable lost groups
				Obsd.	Calcd.		
1	Ⅰ	121.37~181.37	163.37	4.55	5.41	173.37	$1.5H_2O$
	Ⅱ	181.37~251.37	195.87	21.49	—	225.87	*D*-Hhpg and part of nitrate anion
	Ⅲ	251.37~481.37	301.87	24.51	—	299.37	
	Ⅳ	>481.37	340.87	8.50	—	—	—
2	Ⅰ	124.38~159.38	150.38	7.39	7.09	173.88	$2H_2O$
	Ⅱ	159.38~180.88	167.38	2.90	—	193.38	2 nitrate anion
	Ⅲ	180.88~256.88	194.88	21.02	—	224.38	
	Ⅳ	>256.88	336.38	30.16	—	—	—

were a strong exothermic peak (195.87 ℃) and a weak exothermic peak (301.87 ℃) on the DSC curve, corresponding to the decomposition and degradation D-Hhpg and part of nitrate anion. The fourth decomposition steps took place at the temperature of 481.37 ℃, and until 850 ℃ no platform appeared, which indicates that the compound has not completely lost weight.

Compound **2** is relatively stable before 124.38 ℃. The first weight loss in the temperature range of 124.38~159.38 ℃ is consistent with the removal of two lattice water molecules (Obsd. 7.39%, Calcd. 7.09%). On the DSC curve, endothermic peak was observed at about 173.88 ℃, which can prove the decomposition of one and two lattice water molecules. The second and third decomposition steps occurred in a temperature range of 159.38~180.88 ℃ and 180.88~256.88 ℃ with a weight loss of 2.90% and 21.02%, respectively, against calculated weight loss of 24.42%, corresponding to the loss of two nitrate anion. There were a weak exothermic peak (167.38 ℃) and a strong exothermic peak (194.88 ℃) on the DSC curve, corresponding to the decomposition two nitrate anion. The fourth decomposition steps took place at the temperature of 256.88 ℃, and no platform appeared until 850 ℃, indicating that the compound has not completely lost weight.

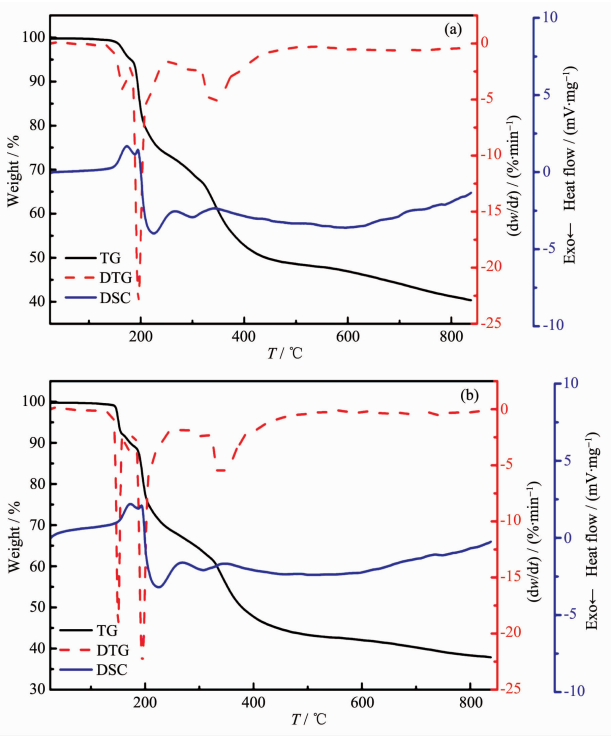

Fig.8　TG-DTG and DSC curves of compounds **1** (a) and **2** (b)

2.5　Cyclic voltammetry

We investigated the electrochemical behavior of the compounds by cyclic voltammetry (CV). Typically, the carbon paste electrodes modified by **1** and **2** were constructed and then electrochemical properties were studied in 1 mol·L^{-1} H_2SO_4 solution at different scan rates in a voltage range of −0.75~1.00 V. It can be seen that the potential of oxidation peak increased and that the potential of reduction peak decreased with the scan rate increasing (Fig.9a,c). Analysis of cyclic voltammetry at varying scan rates (0.03~0.13 V·s^{-1}) demonstrates a linear relationship between the anode peak Ⅰ (or anodic peak Ⅰ′) current and the scan rate (Fig.9b,d), indicating a surface-controlled electrochemical process.

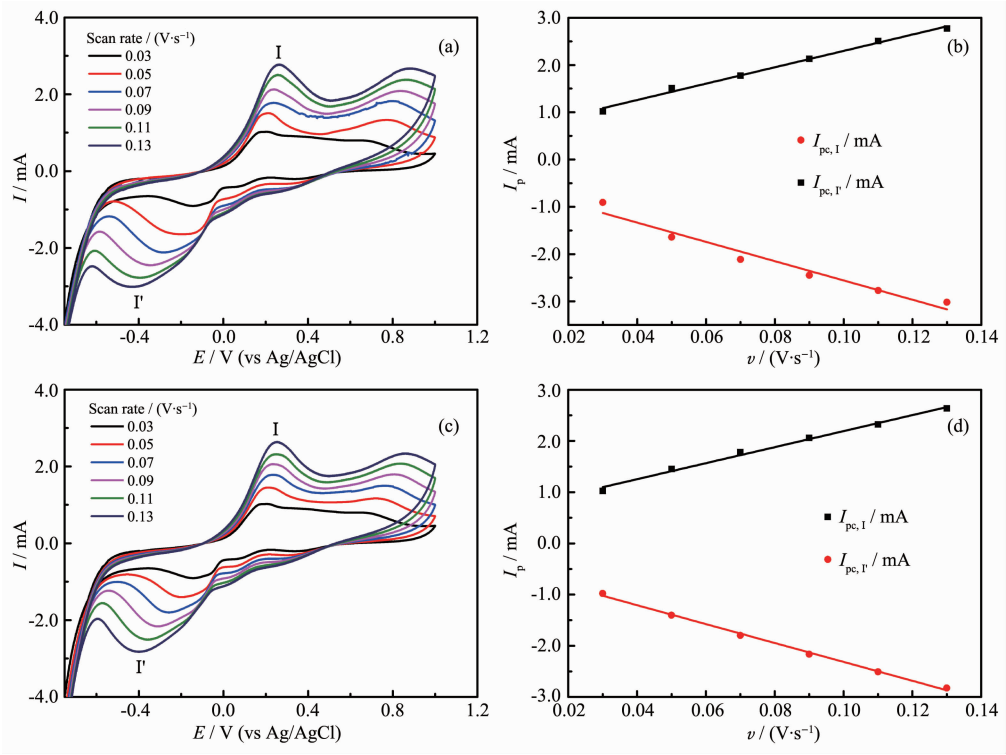

Fig.9 Cyclic voltammograms of compounds **1** (a) and **2** (c); Change of anodic and anode current (I_a) vs scan rate for compounds **1** (b) and **2** (d)

3 Conclusions

In summary, one pair of chiral coordination compounds {[Cu(*D*-hpg)(phen)(NO_3)]·1.5H_2O}$_n$ (**1**) and {[Cu(*L*-hpg)(phen)(NO_3)]·2H_2O}$_n$ (**2**) have been described in detail. They are 1D chain structure, which is extended into a 3D supramolecular structure by the hydrogen bond. Interestingly, for compounds **1** and **2**, there exist left-handed or right-handed supramolecular helix chains along the *b* axis direction by the hydrogen bond, respectively, which is extended by the hydrogen bond between coordinated nitrate anion and lattice water. The TG-DTG and DSC curves reveal that the frameworks of compounds **1** and **2** are thermally stable before 120 ℃. These phenomenon may be attributed to the coexistence of strong hydrogen bonding interaction, π-π stacking interaction and coordination interaction. The cyclic voltammetry of the compounds at varying scan rates (0.03~0.13 V·s^{-1}) demonstrates a linear relationship between the anode peak Ⅰ (or anodic peak Ⅰ′) current and the scan rate, indicating a surface-controlled electrochemical process.

References:

[1] Asnaghi D, Corso R, Larpent P, et al. *Chem. Commun.*, **2017**,**53**:5740-5743

[2] Puglisi R, Ballistreri F P, Gangemi C M A, et al. *New J. Chem.*, **2016**:911-915

[3] Xu Z X, Liu L, Zhang J. *Inorg. Chem.*, **2016**,**55**:6355-6357

[4] Inoue K, Kikuchi K, Ohba M, et al. *Angew. Chem. Int. Ed.*, **2003**,**115**:4958-4961

[5] Seo J S, Whang D, Lee H, et al. *Nature*, **2000**,**404**:982-986

[6] Li M Y, Wang F, Gu Z G, et al. *RSC Adv.*, **2017**,**7**:4872-4875

[7] Shi Z, Qin L, Zheng H. *Dalton Trans.*, **2017**,**46**:4589-4594

[8] Yadav M, Bhunia A, Jana S K, et al. *Inorg. Chem.*, **2016**,**55**:2701-2708

[9] Liu M J, Yuan J, Zhang Y Q, et al. *Dalton Trans.*, **2017**,**46**:13035-13042

[10]Ogasawara M, Wu W Y, Arae S, et al. *Angew. Chem. Int. Ed.*, **2012**,**51**(12):2951-2955

[11]Yousuf I, Arjmand F. *J. Photochem. Photobiol. B*, **2016**,**164**:83-95

[12]Jammi S, Rout L, Saha P, et al. *Inorg. Chem.*, **2008**,**47**:5093-5098

[13]Lewis K G, Ghosh S K, Nattamai B, et al. *ACS Cent. Sci.*,

2015,**1**:50-56

[14]Deiana M, Pokladek Z, Dudek M, et al. *Phys. Chem. Chem. Phys*., **2017**,**19**:21272-21275

[15]Chen L J, Yang H B, Shionoya M. *Chem. Soc. Rev*., **2017**, **46**:2555-2576

[16]Srinivasan S, Athappan P, Rajagopal G. *Transition Met. Chem.*, **2001**,**26**:588-593

[17]Park K H, Noh T H, Shim Y B, et al. *Chem. Commun.*, **2013**,**49**:4000-4002

[18]Kuang R, Zheng L, Chi Y, et al. *RSC Adv*., **2017**,**7**:11701-11706

[19]Feng Q, Yan M J, Song H H, et al. *Inorg. Chim. Acta*, **2014**,**415**:75-80

[20]Zhang S Y, Li D, Guo D, et al. *J. Am. Chem. Soc*., **2015**, **137**:15406-15409

[21]Liu M J, Yuan J, Zhang Y Q, et al. *Dalton Trans*., **2017**,**46**: 13035-13042

[22]Martin N P, Volkringer C, Falaise C, et al. *Cryst. Growth Des*., **2016**,**16**:3785-3790

[23]Mon M, Grancha T, Verdaguer M, et al. *Inorg. Chem.*, **2016**, **55**:6845-6847

[24]Xiao Y Y, Fang H C, Gu Z G, et al. *Cryst. Growth Des*., **2011**,**11**:2824-2828

[25]Cheng M, Wang Q, Bao J, et al. *New J. Chem.*, **2017**,**41**: 5151-5160

[26]Liu G X, Huang H, Chu Q, et al. *Cryst. Growth Des*., **2008**, **8**:3233-3245

[27]Wu L L, Song H H, He R, et al. *Inorg. Chim. Acta*, **2013**, **399**:6-11

[28]Xing A P, Bai C B, Wang L L. *Tetrahedron*, **2013**,**69**:455-459

[29]Rich J, Rodríguez M, Romero I, et al. *Dalton Trans*., **2009**, **38**:8117-8126

[30]Lin J W, Thanasekaran P, Chang J S, et al. *CrystEngComm*, **2013**,**15**:9798-9810

[31]Huang J H, Hou G F, Mad S, et al. *RSC Adv*., **2017**,**7**: 18650-18657

[32]Cao L H, Wei Y L, Yang Y, et al. *Cryst Growth Des*., **2014**, **14**:1827-1838

[33]Liu T, Yu Y H, Zhang H Z, et al. *Cryst Growth Des*., **2017**, **17**:1788-1795

[34]Yue Q, Huang Q, Gao Y Y, et al. *Inorg. Chim. Acta*, **2016**, **443**:110-117

[35]Mukhopadhyay U, Choquesillo-Lazarte D, Niclós-Gutiérrez J, et al. *CrystEngComm*, **2004**,**6**:627-632

[36]Sun M L, Zhang X, Yao Y G. *Synth. React. Inorg. Met.-Org. Chem*., **2015**,**45**:1834-1838

[37]Shi Y J, Song H H. *Inorg. Chim. Acta*, **2018**,**471**:66-75

[38](a)Sheldrick G M. *SHELXS*-97, *Program for Crystal Structure Refinemen*t, University of Göttingen, Germany, **1997**.

(b)Sheldrick G M. *Acta Crystallogr. Sect. A*: *Found. Crystallogr.*, **2008**,**64**:112-122

[39]Speed S, Font-Bardía M, Salah El Fallah M, et al. *Dalton Trans*., **2014**,**43**:16919-16927